Carbohydrate Polymers 186 (2018) 420–428

Contents lists available at ScienceDirect

Carbohydrate Polymers

journal homepage: www.elsevier.com/locate/carbpol

Bioconversion of chitosan into chito-oligosaccharides (CHOS) using family 46 chitosanase from *Bacillus subtilis* (*Bs*Csn46A)

Phornsiri Pechsrichuang[a], Silje B. Lorentzen[b], Berit B. Aam[c], Tina R. Tuveng[b], Anne G. Hamre[b], Vincent G.H. Eijsink[b], Montarop Yamabhai[a,*]

[a] *Molecular Biotechnology Laboratory, School of Biotechnology, Institute of Agricultural Technology, Suranaree University of Technology, Nakhon Ratchasima, 30000, Thailand*

[b] *Department of Chemistry, Biotechnology and Food Science, Norwegian University of Life Sciences (NMBU), P.O. Box 5003, 1432 Ås, Norway*

[c] *BioCHOS AS, co/Incubator Ås, P.O. Box 19, 1431 Ås, Norway*

ARTICLE INFO

Keywords:
GH46
Chitosanase
Bioconversion
Chitosan
Chito-oligosaccharides
Bacillus

ABSTRACT

*Bs*Csn46A, a GH family 46 chitosanase from *Bacillus subtilis* had been previously shown to have potential for bioconversion of chitosan to chito-oligosaccharides (CHOS). However, so far, in-depth analysis of both the mode of action of this enzyme and the composition of its products were lacking. In this study, we have employed size exclusion chromatography, ^{1}H NMR, and mass spectrometry to reveal that *Bs*Csn46A can rapidly cleave chitosans with a wide-variety of acetylation degrees, using a non-processive *endo*-mode of action. The composition of the product mixtures can be tailored by varying the degree of acetylation of the chitosan and the reaction time. Detailed analysis of product profiles revealed differences compared to other chitosanases. Importantly, *Bs*Csn46A seems to be one of the fastest chitosanases described so far. The detailed analysis of preferred *endo*-binding modes using $H_2{}^{18}O$ showed that a hexameric substrate has three productive binding modes occurring with similar frequencies.

1. Introduction

Chito-oligosaccharides (CHOS) can be produced by enzymatically or chemically from chitosans, linear heteropolymers of β(1 → 4) linked *N*-acetyl-D-glucosamine (GlcNAc or A) and D-glucosamine (GlcN or D) (Aam et al., 2010). Such chitosans are produced from chitin, one of Nature's primary structural polysaccharides, found in the outer exoskeleton of arthropods (of which crabs, lobster and shrimps are of importance for industrial production of chitosan) and in fungal cell walls. Chitin is an abundant bioresource that needs proper bioremediation, and its value-creating conversion to chitosan and CHOS is thus of major interest (Khoushab & Yamabhai, 2010). Chitosans differ in terms of their chain length (degree of polymerization, DP), fraction of acetylation (F_A), and pattern of acetylation (P_A). The F_A needs to be below 0.7 for the chitosan to be soluble. Chitosans that are generated by de-*N*-acetylation of chitin under homogeneous conditions have a random distribution of A- and D- subunits (Vårum, Antohonsen, Grasdalen, & Smidsrød, 1991).

Chitosanases, or chitosan *N*-acetylglucosaminohydrolases (EC 3.2.1.132), catalyzes the hydrolysis of glycosidic bonds in chitosan, and limited hydrolysis will lead to the production of CHOS (Fukamizo, Ohkawa, Ikeda, & Goto, 1994). CHOS have various potential applications in the food, agricultural and pharmaceutical industries and there is increasing interest in the conversion of chitin, via chitosan into bioactive CHOS (Aam et al., 2010; Xia, Liu, Zhang, & Chen, 2011). Enzymatic conversion of chitosan is attractive since this leads to clean processes and because there is a wide variety of depolymerizing enzymes with varying cleavage specificities. Thus, by varying the enzyme, different product mixtures can be obtained. Enzymes with chitosanase activity have been found in various glycosyl hydrolase (GH) families according to the CAZy database, and there are three families that only have chitosanases: GH46, GH75, and GH80. Notably, chitosan contains four types of glycosidic bonds: D-D, A-A, D-A and A-D. Chitosanases will differ in their preferences for these pairs of monomers, and these

Abbreviations: *Bs*Csn46A, GH family 46 chitosanase from *Bacillus subtilis*; CHOS, chito-oligosaccharides; GlcNAc or A, N-acetyl-D-glucosamine; GlcN or D, D-glucosamine; DP, degree of polymerization; F_A, fraction of acetylation; P_A, pattern of acetylation; GH, glycosyl hydrolase; CAZy, carbohydrate-active enZYmes; SEC, size exclusion chromatography; MS, mass spectrometry; RI, refractive index; MALDI TOF/TOF MS, Matrix-Assisted Laser Desorption Ionization mass spectrometry; DP_n, average degree of polymerization; AMAC, 2-aminoacridone; DHB, 2,5dihydroxybenzoic acid; MW_n, average molecular weight

* Corresponding author.

E-mail addresses: phornsiri.p@gmail.com (P. Pechsrichuang), silje.lorentzen@nmbu.no (S.B. Lorentzen), berit.aam@nmbu.no (B.B. Aam), tina.tuveng@nmbu.no (T.R. Tuveng), anne.grethe.hamre@nmbu.no (A.G. Hamre), vincent.eijsink@nmbu.no (V.G.H. Eijsink), Montarop@g.sut.ac.th (M. Yamabhai).

https://doi.org/10.1016/j.carbpol.2018.01.059
Received 20 October 2017; Received in revised form 13 January 2018; Accepted 17 January 2018

preferences may also be affected by adjacent sugars. Enzymes with a preference for A–A would be classified as chitinases (families GH18 and GH19), but these enzymes also act on chitosan (Horn et al., 2006a; Itoh et al., 2002; Purushotham, Sarma, & Podile, 2012; Sørbotten, Horn, Eijsink, & Vårum, 2005; Stefanidi & Vorgias, 2008).

In a previous study, we expressed a family 46 chitosanase (Takasuka et al., 2014; Viens, Lacombe-Harvey, & Brzezinski, 2015) from *Bacillus subtilis* strain 168 (*Bs*Csn46A; UniProt: CHIS_BACSU; locus name BSU26890). Basic characterization of the enzyme revealed industrially relevant properties such as high thermostability and pH-stability, high-level secretory expression in *Escherichia coli*, and the ability to convert chitosan (Pechsrichuang, Yoohat, & Yamabhai, 2013). This enzyme belongs to group B of the GH46 chitosanases, according to a phylogenetic analysis carried out by Viens et al. (2015), for which there is not yet a representative that has been characterized in-depth. Because of this and because of promising initial results, we have now carried out an in-depth analysis of the mode of action of this enzyme. Furthermore, we have analyzed its ability to convert chitosan in detail, including an analysis of the composition and sequence of its hydrolytic products. These analyses were carried out using state-of-the-art size exclusion chromatography (SEC), ^{1}H NMR and mass spectrometry (MS) methods. We have carried out conversion reactions with various types of chitosans, leading to a variety of product mixtures.

2. Materials and methods

2.1. Chitosans

Kitoflokk™ chitosan with F_A 0.15 and an average DP (DP_n) of approximately 206 (corresponding to an average molecular weight (MW_n) of 37 kDa) was provided by Teta Vannrensing (Kløfta, Norway). Chitosan with F_A 0.3 and DP_n > 1000, (MW_n = 200–400 kDa) was purchased from Heppe Medical chitosan GmbH (Halle, Germany). Highly acetylated chitosan with F_A 0.6 was prepared by homogenous de-*N*-acetylation of chitin from shrimp shells (Chitonor, Senjahopen, Norway), according to a previously described method (Sannan, Kurita, & Iwakura, 1975; Vårum et al., 1991). Briefly, 4 g of chitin flakes was mixed with 100 g of 40% (w/v) NaOH and incubated at 4 °C overnight. Then, 300 g of ice was added and the solution was stirred until homogeneous. Undissolved chitin was removed by centrifugation (10000*g* at 4 °C). After sparging with nitrogen gas for 10 min to remove oxygen, the solution was incubated at 25 °C (water bath) for 42 h to deacetylate chitosan. The deacetylation reaction was stopped by adding 280 g of ice. The solution was stirred until it was homogeneous, followed by addition of HCl until the pH reached 4.5. The chitosan sample was dialyzed against water using a dialysis membrane with 12–14 kDa cut-off (SpectrumLabs, Texas, USA) to remove salt. The water was changed several times until the conductivity reached 3 μS. The resulting chitosan solution was then filtered (Whatman filters, first 1.2 μM, then 0.8 μM; Millipore) and lyophilized.

2.2. Expression of recombinant BsCsn46A gene in E. coli

A gene fragment encoding *Bs*Csn46A was engineered for secretory production in *E. coli*, as previously described (Pechsrichuang et al., 2016; Pechsrichuang et al., 2013). To produce the enzyme, a single colony of freshly transformed *E. coli* TOP10 harboring the OmpA-Csn/pMY202 (Pechsrichuang et al., 2016) was grown in Luria Bertani (LB) broth containing 100 μg/ml ampicillin (LB-Amp) overnight, at 37 °C, with shaking at 180 rpm. Then 5 ml of the overnight cultures was used to inoculate 0.5 L of ampicillin containing TB medium, and bacteria grown in airlift fermenter (Harbinger Biotechnology and Engineering, Ontario, Canada) at 37 °C until the OD_{600} reached 1.0. At that point, isopropyl-β-D-thiogalactopyranoside (IPTG) was added to a final concentration of 0.1 mM, and the incubation was continued at 28 °C for 20 h. The culture broth was collected by centrifugation at 4000*g* for 30 min at 4 °C and concentrated using a VivaFlow 200 system equipped with a filter with a molecular weight cut-off (MWCO) of 10000 Da. The recombinant chitosanase, containing C-terminal His_{10} tag, was purified by immobilized metal affinity chromatography (IMAC), using Ni-NTA agarose, according to the manufacturer's instruction (Qiagen, Hilden, Germany).

2.3. Enzymatic degradation of chitosan

Chitosans with different fractions of acetylation (F_A 0.15, 0.3 and 0.6) were dissolved in 40 mM sodium acetate buffer, pH 5.5, containing 100 mM NaCl and 0.1 mg BSA/ml of chitosan. Chitosan solutions F_A 0.15 and 0.3 (final concentration of 10 mg/ml) were pre-incubated in an incubator shaker at 37 °C, and the degradation reactions were started by adding 0.05 μg of *Bs*Csn46A per mg of chitosan. Samples were taken from the reactions at various time points from 10 min to 2880 min. The reaction was stopped by adding 150 μl of 1 M HCl followed by heating at 100 °C for 3 mins. Then, the samples were concentrated and dried by using a vacuum concentrator. Before ^{1}H NMR, the samples were dissolved in D_2O and the pD was adjusted to 4.5. Alternatively, the samples were dissolved in 0.15 M ammonium acetate, pH 4.5, for SEC. To increase the degrees of scission (α) of chitosans, additional of *Bs*Csn46A was added at 0.05 μg per mg of chitosan after incubation for 1440 min, and the degradation reaction was continued for 1440 min.

For high acetylated chitosan (F_A 0.6), the degradation reactions were started by adding 4 μg of the enzyme per mg of chitosan and incubated at 50 °C for 1440 min. To increase the α-values of chitosan, more enzyme (4 μg per mg of chitosan) was added and further incubated for 1440 min.

2.4. Size-exclusion chromatography

SEC was used for baseline separation of CHOS as previously described (Sørbotten et al., 2005). Three XK 26 columns were connected in series and packed with Superdex™ 30 (Pharmacia Biotech, Uppsala, Sweden), with an overall dimension of 2.60 × 180 cm. The mobile phase, (0.15 M ammonium acetate, pH 4.5) was pumped through the system using an LC-10ADvp pump (Shimadzu GmbH, Duisburg, Germany) at a flow rate of 0.8 ml/min. Products were detected using a refractive index (RI) detector (Shodex RI-101, Shodex Denko GmbH, Dusseldorf, Germany) coupled to a CR 510 Basic Data logger (Campbell Scientific Inc., Logan, UT). Fractions of 4 ml were collected using a fraction collector for CHOS sequence analysis.

2.5. NMR spectroscopy

Samples for ^{1}H NMR analysis were dissolved in D_2O, and then DCl or NaOD were used to adjust the pD to 4.3–4.6. ^{1}H NMR spectra were obtained at 400 MHz at a temperature of 85 °C, as previously described (Vårum et al., 1991). The degree of scission (α), which equals the fraction of cleaved glycosidic linkages, was calculated as the inverse value of DP_n (average degree of polymerization). The DP_n was calculated as previously described (Sørbotten et al., 2005), using the formula $DP_n = (A\alpha + A\beta + D\alpha + D\beta + A + D)/(A\alpha + A\beta + D\alpha + D\beta)$. Aα, Aβ, Dα and Dβ equal the integrals of the reducing end signals of α and β anomers of GlcNAc and GlcN, respectively, and A and D equal the integrals of the peaks representing sugars in internal positions and at the non-reducing end. The signals for the β-anomers of reducing end sugars are difficult to quantify because they overlap with the internal signals (for D) or because, in the case of A, they appear as two doublets at 4.705 ppm (–AA) and 4.742 ppm (–DA). Therefore, the β-anomer signals were calculated from the α-anomers signals based on the known α/β anomer ratio of 60:40 (Horn et al., 2006b; Koga, Yoshioka, & Arakane, 1998; Tsukada & Inoue, 1981). The internal signals for D were then corrected.

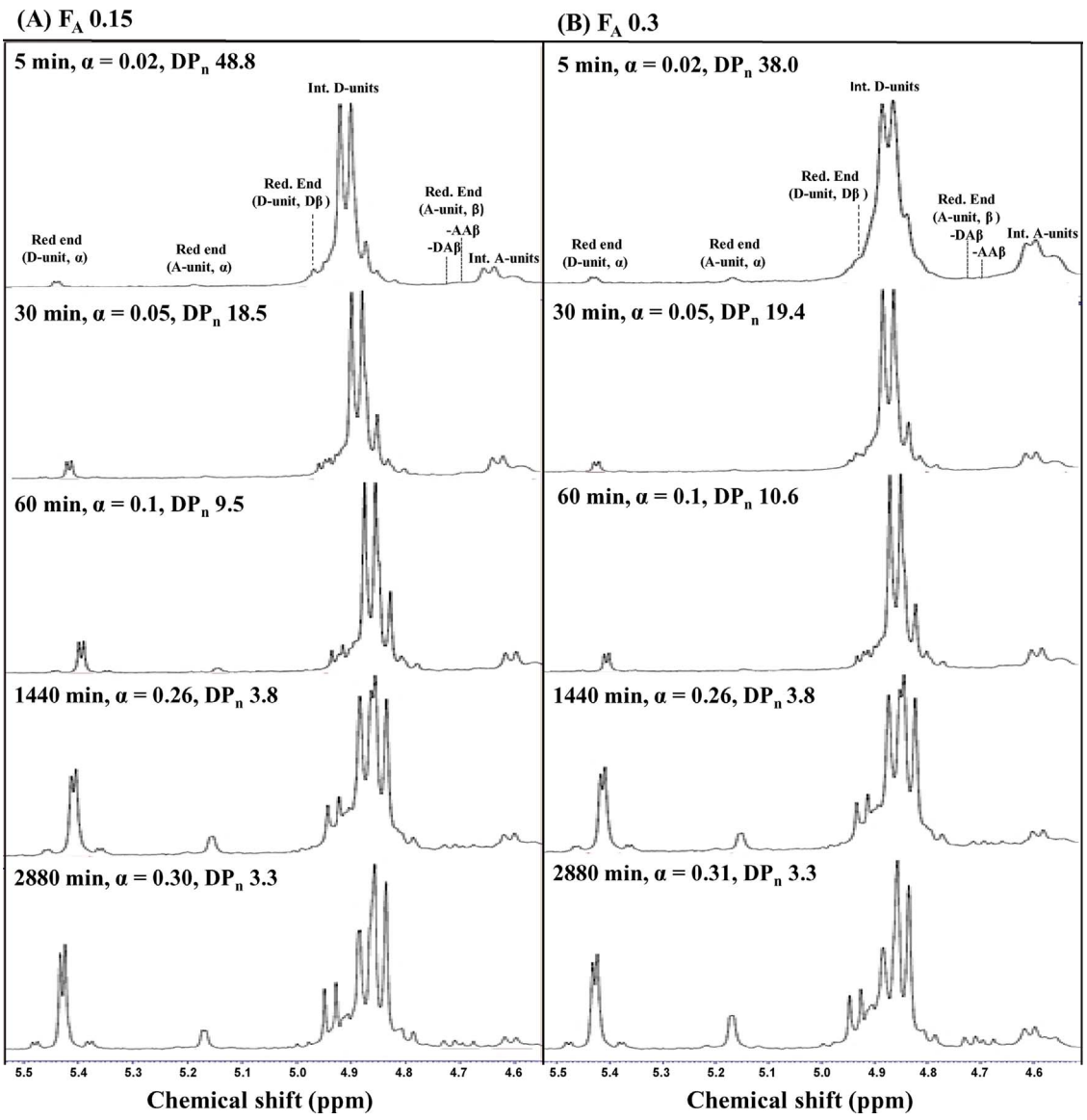

Fig. 1. Product formation over time during degradation of chitosans with F_A 0.15 (left) or F_A 0.3 (right) with *Bs*Csn46A, analyzed by ^{1}H NMR. The figure shows ^{1}H NMR spectra of the anomer region of chitosans with F_A 0.15 or F_A 0.3 at various time points during degradation with *Bs*Csn46A. The α-values (degree of scission) and the DP_n (average chain length in the product mixture) at each time point are indicated. A reducing end D-unit resonates at 5.43 ppm (α-anomer) and 4.92 ppm (β-anomer). The α-anomer of a reducing end A-unit resonates at 5.19, while the β-anomer appears as two doublets at 4.705 ppm (–AA) and 4.742 ppm (–DA), depending on whether the preceding sugar unit is an A or a D, respectively. Internal D-units resonate at 4.8–4.95 ppm, whereas internal A-units resonate at 4.55–4.68. See Sørbotten et al. (2005) and the Materials and Methods section for more details concerning the interpretation and quantification of these spectra.

2.6. Analysis of CHOS by mass spectrometry (MS)

Identification of isolated CHOS was performed with Matrix-Assisted Laser Desorption Ionization mass spectrometry (MALDI TOF/TOF MS). MS spectra were acquired using an UltraflexTM TOF/TOF mass spectrometer (Bruker Daltonik GmbH, Bremen, Germany) with gridless ion optics under the control of Flexcontrol. For sample preparation, 1 μl of sample was mixed with 1 μl of 10% (w/v) 2,5dihydroxybenzoic acid (DHB) in 30% acetonitrile and spotted onto a MALDI target plate (Bahrke et al., 2002). The MS experiments were conducted using an accelerating potential of 20 kV in reflectron mode.

2.7. CHOS sequencing

Approximately 20 mg of CHOS obtained from degradation of F_A 0.3 chitosan to a degree of scission of 0.14 or 0.26 were dried using a vacuum concentrator and separated by SEC as described above. The individual fractions of CHOS obtained from the SEC experiment were lyophilized using a freeze dryer. Then, the CHOS (from DP2 to DP6) were labeled with 2-aminoacridone (AMAC) (Bahrke et al., 2002) and purified using a C-18 column (Starata C18E, Phenomenex, CA, USA) (Morelle, Canis, Chirat, Faid, & Michalski, 2006), as follows. The CHOS typically 0.5 mg were dissolved in 10 μl of 0.1 M of AMAC and 10 μl of 1 M natriumcyanoborhydride (NCBH). The samples were heated at 90 °C for 30 min (in the dark), cooled to −20 °C, and dried using a vacuum concentrator. The dried samples were dissolved in 100 μl of 70% methanol and centrifuged at 10000*g* for 30 min to remove undissolved CHOS. Then, the samples were dried using the vacuum concentrator and dissolved in 100 μl deionized water. After centrifuge for 5 min to remove possible particles the sample was applied to a C-18 column (Starata C18E, Phenomenex, CA, USA), which was used for purification of AMAC-labeled CHOS. The eluted AMAC-labeled CHOS were dried using the vacuum concentrator and stored at −20 °C until analysis. Before analysis the samples were dissolved in 50 μl of 50%

methanol. Analysis was performed using an LTQ-Velos Pro ion trap mass spectrometer (Thermo Scientific, Bremen, Germany) connected to an Ultimate 3000 RS HPLC (Dionex, CA, USA), using a setup for direct injection without a column. The pump delivered 200 μl/min of 0.03 μM formic acid in 70% acetonitrile and the data was acquired for 24 s after injection. The capillary voltage was set to 3.5 kV and the scan range was *m/z* 150–2000 using two micro scans for the MS. The automatic gain control was set to 10,000 charges and a maximum injection time of 20 milliseconds. For fragmentation of desired precursor masses by MS2, the normalized collision energy was set to 37 and three micro scans were used. The data were recorded with Xcalibur version 2.2.

2.8. Hydrolysis of $(GlcN)_5$ and $(GlcN)_6$ in $H_2{}^{18}O$ for subsite mapping

To determine preferred binding modes for the substrate, hydrolysis of $(GlcN)_5$ and $(GlcN)_6$ was carried out in $H_2{}^{18}O$ (Larodan Fine Chemicals, Malmö, Sweden), as previously described (Eide, Lindbom, Eijsink, Norberg, & Sørlie, 2013; Hekmat et al., 2010). In accordance with the previously published protocols, reactions were set up with such as to reach approximately 20% substrate conversion in short reaction times (up to two minutes). Short reaction times are needed to avoid non-enzymatic incorporation of ^{18}O, as described by Eide et al. (2013). The enzyme concentration was adjusted to ensure that 20% substrate conversion happened within the first two minutes. The enzyme stock solutions were highly concentrated to keep the volume of added enzyme and, thus, unlabeled H_2O, below 2% of the total reaction volume (Hekmat et al., 2010). The hydrolysis was performed at 37 °C and 600 rpm in $H_2{}^{18}O$ containing 50 mM sodium acetate buffer (pH 5.5) and 5 mM $(GlcN)_5$ or $(GlcN)_6$. Reactions were started by adding enzyme to a final concentration of 1.8 μM and 1.4 μM for the reactions with $(GlcN)_5$ and $(GlcN)_6$, respectively. Samples of 1 μl were taken at several time points within the first 120 s of the reaction. The reactions were immediately quenched by mixing with a DHB solution (15 mg/ml DHB in 30% ethanol), spotted directly on the MALDI target and dried. The hydrolysis products were then analyzed by MALDI-TOF-MS as previously described (Eide et al., 2013). Data were analyzed for the time point where approximately 20% of the substrate had been converted. The minor errors caused by the presence of unlabeled water and non-enzymatic incorporation of ^{18}O were neglected.

3. Results and discussion

3.1. Hydrolysis of chitosan

^1H NMR spectroscopy was used to analyze the time course of the degradation of chitosan with F_A 0.15 or F_A 0.3. NMR spectra of the product mixtures were recorded at several time points during the degradation reaction and were assigned as described in Sørbotten et al. (2005) (see also Ishiguro, Yoshie, Sakurai, and Inoue (1992) and the Materials and Methods section for further details). The spectra, depicted in Fig. 1, show that the new reducing ends generated early in the reaction were almost exclusively deacetylated (D). At early time points, the spectra show signals at 5.43 ppm and 4.92 ppm, representing the α and β anomers of a reducing end D, respectively, while signals representing acetylated reducing ends (A; 5.19 ppm and 4.742 ppm) only appeared after more extensive degradation (α-values above 0.1). Thus, *Bs*Csn46A has an expected preference for D-units in the −1 subsite, although the enzyme can also hydrolyze glycosidic linkages following an A-unit. Reducing end A units give multiple signals: the α-anomer resonates at 5.19 ppm, whereas the β-anomer of a reducing end A resonates at 4.705 or 4.742 ppm, depending on whether the preceding unit is an A or a D, respectively (Sørbotten et al., 2005). The fact that only the 4.742 ppm signal was observed indicates that cleavage after an A only occurs if the preceding unit is deacetylated.

Progress curves for the degradation of the chitosans, i.e. curves showing the increase in α over time (Fig. 2), showed a rapid linear phase until the α-values reached 0.15–0.20, followed by a slower second phase at higher α-values. Reactions set-up to yield maximum degradation of the chitosans gave maximum α-values of 0.30 and 0.31 for F_A 0.15 and F_A 0.3, respectively, which means that about 1 in 3 of the glycosidic bonds had been cleaved. Interestingly, the maximum α-value obtained with the F_A 0.3 chitosan is considerably lower than the maximum α-value of 0.44 obtained when degrading a F_A 0.32 chitosan with ScCsn46A, a family 46 chitosanase from *Streptomyces coelicolor* A3(2) (Heggset et al., 2010).

Using five data points recorded during the first hour of the reaction (Fig. S1), the initial specific activity was then calculated as previously described (Heggset, Hoell, Kristoffersen, Eijsink, & Vårum, 2009). The initial specific activity of *Bs*Csn46A was 5.5×10^3 and 8.4×10^3 min^{-1} for F_A 0.15 and F_A 0.3, respectively. The initial rates displayed by *Bs*Csn46A are remarkably high. Previous studies have shown that degradation of a chitosan with F_A 0.32 by ScCsn46A (Heggset et al., 2010) or of a chitosan with F_A 0.31 by SaCsn75A from *Streptomyces avermitilis* (Heggset et al., 2012) have initial rates of 325 min^{-1} and 6.5 min^{-1}, respectively. This result confirms indications from previous studies which concluded that *Bs*Csn46A has high potential for biotechnological applications (Pechsrichuang et al., 2016; Pechsrichuang et al., 2013). It is remarkable that the initial specific activity of *Bs*Csn46A against F_A 0.3 chitosan was approximately 1.5 times higher compared to the F_A 0.15 chitosan. Likewise, it was unexpected that the enzyme reaches almost identical α-values for the two substrates, despite the difference in acetylation. This could be due to binding preferences of the enzyme for certain sequences containing acetylated sugars, but could also reflect a difference in the substrates. The substrates may differ in terms of the randomness of the distribution of acetylated units and this can affect hydrolysis yields. Notably, when increasing the F_A to 0.6, hydrolysis yields in terms of maximum α decreased to approximately 0.18 as indicated by SEC experiment in the next section (Fig. 3C), in line with the notion that *Bs*Csn46A is a chitosanase and not a chitinase.

3.2. Size distribution of CHOS obtained after degradation of chitosans with varying degrees of acetylation

CHOS mixtures were separated by size exclusion chromatography (SEC) as shown in Fig. 3. The chromatograms indicated size distributions of oligomers obtained after degradation of chitosans with F_A 0.15, 0.3 or 0.6 at two α-values, one intermediate value and one at approximately maximum α. The DP of the peaks was assigned using MALDI-TOF MS. The chromatograms showed rapid disappearance of the polymer peak (not shown) and production of a continuum of odd- and even-numbered oligomers, indicating that *Bs*Csn46A is a non-processive *endo*-acting enzyme, similar to ScCsn46A and SaCsn75A (Heggset et al., 2010; Heggset et al., 2012).

In the initial phase of the reactions with chitosans with F_A 0.15 and F_A 0.3 the dominating products were oligomers in the DP3–DP6 range, whereas DP2 and longer oligomers up to a DP of approximately 15 were produced. After extensive degradation, the amount of the short oligomers increased and the main products were dimers and trimers. No monomers were observed, confirming previous TLC analyses (Pechsrichuang et al., 2013). Interestingly, the chromatograms showed that, at the end of the reaction, the amount of DP6 was higher than the amount of DP5. This product profile is unique to *Bs*Csn46A and further illustrates the difference with ScCsn46A (Heggset et al., 2010), which produces more pentamer than hexamer, is slower and reaches higher α-values.

Hydrolysis of the F_A 0.6 chitosan yielded a continuum of products reaching from DP3 to DP > 10 (Fig. 3C). Clearly, *Bs*Csn46A generates many longer non-cleavable oligomeric products. In this case, as expected (Heggset et al., 2010), the dimer top was clearly split into two, reflecting the presence of considerable amounts of acetylated dimers.

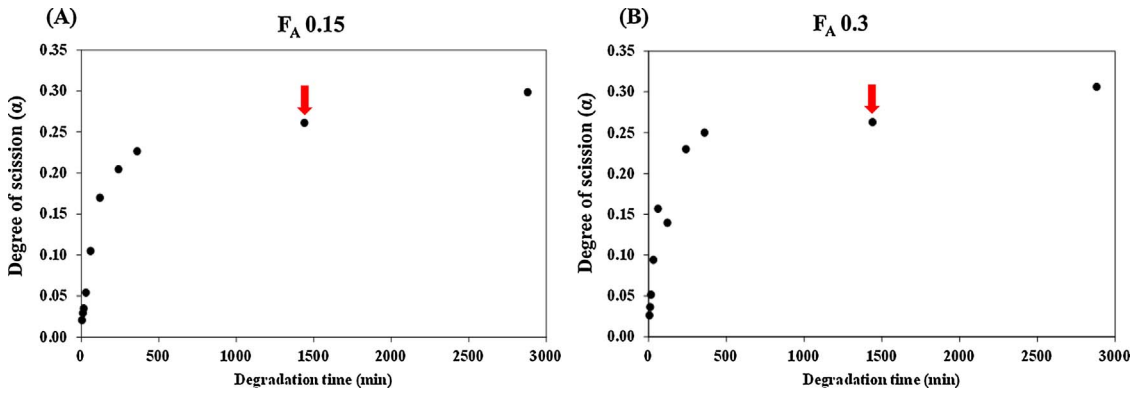

Fig. 2. Time-course for the increase in α during degradation of chitosans with F_A 0.15 (left) or F_A 0.3 (right) with *Bs*Csn46A. The graph shows the degree of scission (α) determined by ^{1}H NMR in reactions containing 10 mg/ml chitosan, 0.05 μg of *Bs*Csn46A per mg of chitosan in 40 mM sodium acetate buffer, pH 5.5, containing 100 mM NaCl and 0.1 mg BSA/ml of chitosan. In an attempt to reach maximum conversion of the chitosans, additional *Bs*Csn46A was added at 0.05 μg per mg of chitosan after incubation for 1440 min (red arrow), and the degradation reaction was continued for another 1440 min (For interpretation of the references to colour in this figure legend, the reader is referred to the web version of this article.)

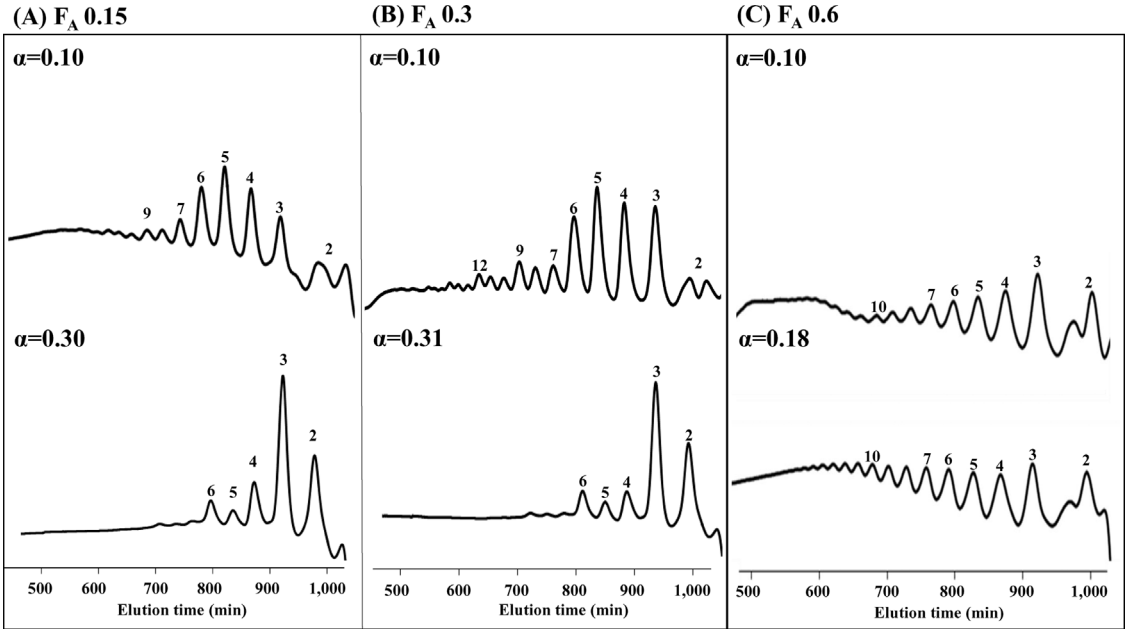

Fig. 3. Product analysis by size exclusion chromatography (SEC). Size distribution of CHOS after degradation of three different chitosans at 37 °C for F_A0.15 and F_A 0.3 chitosans and 50 °C for F_A 0.6 chitosan using *Bs*Csn46A. For each chitosan an intermediate product mixture (α = 0.10) and a final product mixture (varying α) is shown. The peaks are labeled with the DP values.

Table 1
Chemical composition of CHOS fractions[a].

DP	F_A 0.15		F_A 0.3		F_A 0.6
	α = 0.12	α = 0.30	α = 0.11	α = 0.31	α = 0.18
2	**D2**, DA, A2	**D2**, DA, A2	**D2**, DA, A2	**D2**, DA, A2	**DA**, A2, D2
3	**D3**, **D2A1**, D1A2	**D3**, **D2A1**, D1A2	**D3**, **D2A1**, D1A2	**D3**, **D2A1**, D1A2	**D2A1**, D1A2, D3, A3
4	**D4**, D3A1, D2A2, D1A3	**D4**, D3A1, D2A2	**D4**, D3A1, D2A2, D1A3	**D3A1**, D4, D2A2,D1A3	**D2A2**, D1A3, D3A1
5	**D5**, D4A1, D3A2, D2A3	**D4A1**, D3A2, D2A3	**D5**, D4A1, D3A2, D2A3, D1A4	**D4A1**, D3A2, D2A3	**D2A3**, D3A2, D1A4, D4A5
6	**D6**, D5A1, D4A2, D3A3, D2A4	**D5A1**, D4A2, D3A3	**D6**, D5A1, D4A2, D3A3	**D5A1**, D4A2, D3A3, D2A4	**D3A3**, D2A4, D4A2, D1A5
7	**D7**, D6A1, D5A2	NA.	**D7**, D6A1, D5A2, D4A3, D3A4	NA.	**D3A4**, D4A3, D5A2, D1A6

[a] Chemical composition of CHOS fractions obtained after size exclusion chromatography of product mixtures generated by *Bs*Csn46A from chitosans with varying F_A. The bold letters represent seemingly dominant products, defined by using the signal intensities of MS (height of the peak). NA, not analyzed.

3.3. Chemical composition of CHOS fractions obtained after degradation of chitosans with varying F_A

The chemical compositions of individual CHOS fractions obtained after degradation of chitosans with F_A values of 0.15, 0.3, or 0.6 were analyzed by MALDI-TOF-MS and the results are summarized in Table 1. For the chitosans with F_A 0.15 and F_A 0.3, fully deacetylated oligomers were the dominating products in the early phase of the reaction, whereas A-containing products became more dominant after extensive degradation, while D5, D6 and D7 disappeared (Table 1). The dimer

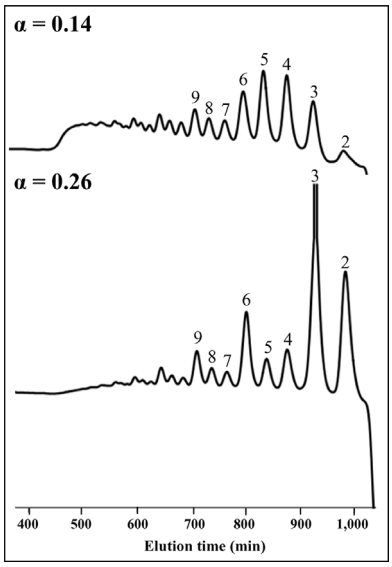

Fig. 4. Size distribution of CHOS for sequence analysis. Chromatograms of CHOS products after degradation of chitosan F_A 0.3 with *Bs*Csn46A to α-values 0.14 and 0.26 at 37 °C are illustrated. These CHOS fractions were isolated for oligomer sequencing. The peaks are labeled with the DP values.

peaks contained a mixture of primarily D2 and DA and a small amount of A2, both in the initial rapid phase and at the end of the reaction. The trimer fraction contained approximately equal amounts of D3 and D2A1 and a small amount of D1A2 both in the initial phase and at the end of the reactions, indicating that *Bs*Csn46A cannot cleave these oligomers. The product compositions obtained upon degradation of the F_A 0.15 and F_A 0.3 chitosans were slightly different, with several A-rich products only being detected in product mixtures generated from the F_A 0.3 chitosan. It is interesting to note that the product mixtures seem to contain pentamers and hexamers that contain only one A. So, in some cases, one internal A unit apparently hampers hydrolysis by *Bs*Csn46A, which is yet another difference of this enzyme compared to ScCsn46A.

As expected, products obtained after extensive degradation of the highly acetylated F_A 0.6 chitosan, contained relatively many acetylated sugars and were longer. Fully deacetylated products longer than D3 were not observed.

3.4. CHOS sequences

To determine the sequences of hydrolytic products, CHOS were produced by degrading F_A 0.3 chitosan to α-values of 0.14 and 0.26, using the same condition as described in Section 2.3, followed by SEC (Fig. 4). The CHOS were derivatized by reductive amination of the reducing end with 2-aminoacridone (AMAC), and the resulting compounds were analyzed by MS/MS, giving insights into CHOS sequences. MS1 and MS2 spectra of CHOS after degradation of the chitosan to α = 0.14 are shown in Fig. S2A and B, while Fig. S3A and B show MS1 and MS2 spectra for the α = 0.26 sample; the results are summarized in Table 2.

For DP3, DP4 and DP5, the MS1 spectra (supplementary Fig. S2A, S3A) showed a dominance of fully and highly deacetylated products at α = 0.14 (supplementary Fig. S2A), and a shift towards products with a higher degree of acetylation at α = 0.26 (supplementary Fig. S3A). MS1 spectra for the hexamer were similar at α = 0.14 and α = 0.26, with a dominance of products carrying two or three acetylations. This is probably due to the fact that intermediate products of this length (hexameric) and with a higher fraction of D are good substrates and thus rapidly cleaved. Somewhat unexpectedly, the dominating dimer at α = 0.14 was DA (dominating sequence DA), whereas at α = 0.26 the dominating dimer was DD, as expected. A plausible explanation is that *Bs*Csn46A is *endo*-acting, i.e. has multiple subsites (see Section 3.5) and

Table 2
Sequences of isolated CHOS[a].

Degree of scission (α)	Degree of polymerization							
	DP2		DP3		DP4		DP5	DP6
	MS1 peak	Sequence from MS2	MS1 peak	Sequence from MS2	MS1 peak	Sequence from MS2	MS1 peak	MS1 peak
0.14	**DA**	**DA**	D2A1	**DDA**	D4	**DDDD**	**D5**	**D4A2**
		AD		DAD	D3A1	**DDDA**	D4A1	D3A3
	D2	DD		ADD		DDAD	D3A2	D5A1
	A2	AA	D3	**DDD**		ADDD	D2A3	D6
			D1A2	**ADA**		DADD	D1A4	
				DAA	D2A2	**DADA**		
				AAD		**DDAA**		
						ADDA		
						AADD		
						ADAD		
						DAAD		
					D1A3	NA.		
0.26	D2	**DD**	D2A1	**DDA**	D3A1	**DDDA**	D3A2	D4A2
	DA	**DA**		ADD		DDAD	D4A1	D5A1
		AD		DAD		DADD	D2A3	D3A3
			D3	DDD		ADDD		D2A4
			D1A2	**ADA**	D1A3	**AADA**		
				DAA		**ADAA**		
				AAD		AAAD		
					D2A2	**ADDA**		
						DDAA		
						DADA		
						ADAD		
						DAAD		
					D4	DDDD		

[a] Analysis of CHOS sequences obtained after size exclusion chromatography of F_A 0.3 chitosan hydrolyzed with *Bs*Csn46A to α-value 0.14 and 0.26. The isolated CHOS (DP2 to DP6) were labeled with AMAC. The oligomer sequences were determined using MS. Sequences in bold are the dominating sequences based on the relative intensity of MS2 signals. MS2 sequence analysis of DP5 and DP6 CHOS was not performed due to the complexity of these samples. NA., not analyzed.

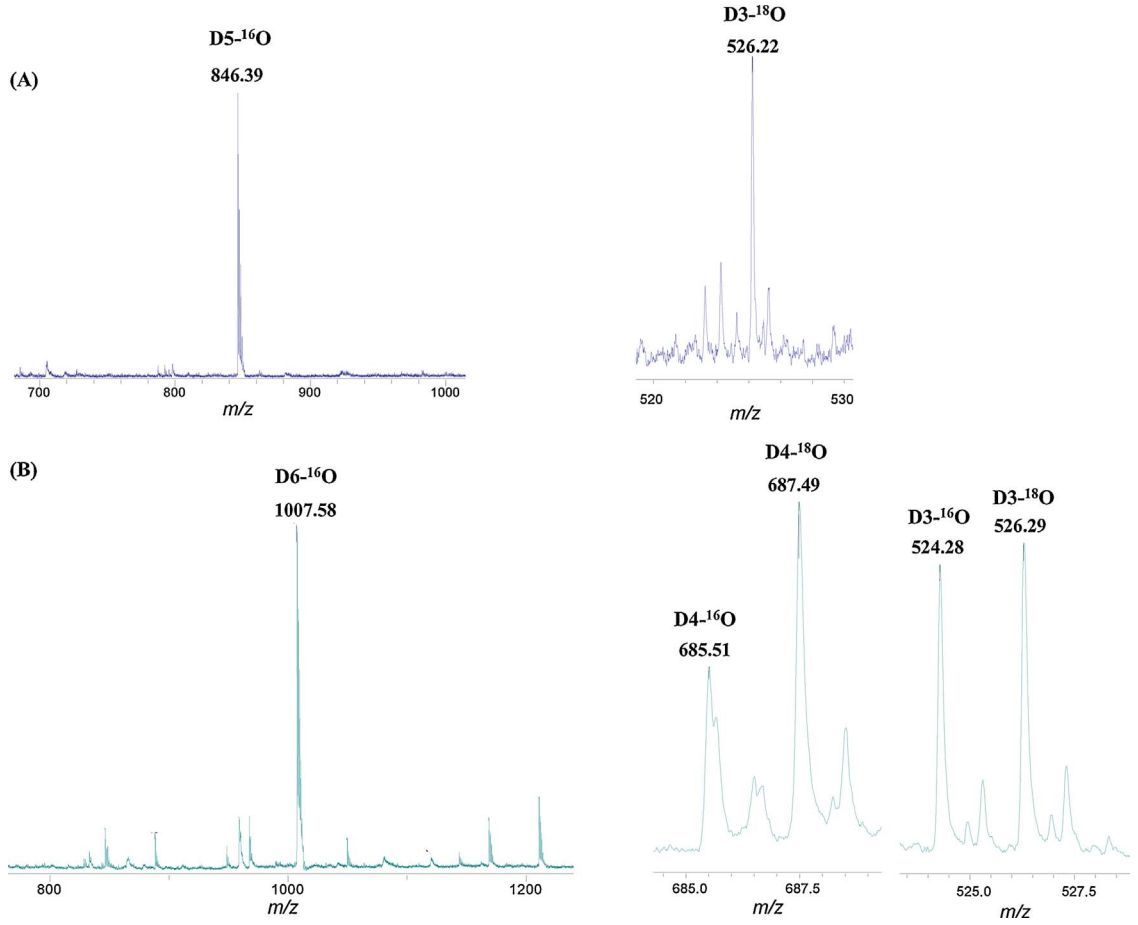

Fig. 5. MALDI-TOF-MS analysis of $(GlcN)_5$ and $(GlcN)_6$ degradation. Products generated from $(GlcN)_5$ (panel A) and $(GlcN)_6$ (panel B) in $H_2{}^{18}O$ are illustrated. The left panel shows the substrate, while key hydrolysis products with ^{16}O and ^{18}O are shown in the right panel. GlcN is abbreviated as D. All labeled peaks are sodium adducts. Dimeric products were not shown.

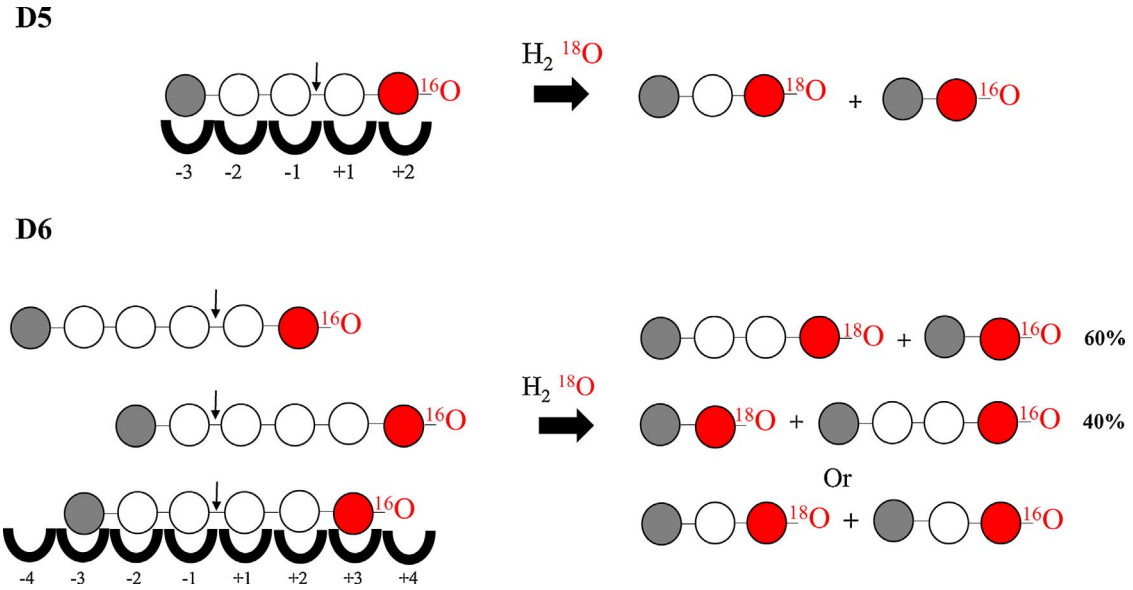

Fig. 6. Productive binding modes of *Bs*Csn46A. Cleavages of $(GlcN)_5$ and $(GlcN)_6$ as derived from experiments with $H_2{}^{18}O$ are depicted. The proposed binding modes and their frequencies were derived from signal intensities (height of the peak) in MALDI-TOF-MS. Grey, red and white circles represent non-reducing end, reducing end and internal GlcN units. (For interpretation of the references to colour in this figure legend, the reader is referred to the web version of this article.)

may thus not be very active on shorter intermediate substrates, which is needed to generate dimeric products. Additionally, one would have to assume that when the substrates become short the enzyme prefers an A to be bound in its −1 subsite (on polymeric substrates, the enzyme cleaves preferably after D, as clearly shown by ^1H NMR in Fig. 1).

MS2 spectra (supplementary Fig. S2B, S3B) showed that for DP3 and DP4, the reducing ends of mono-acetylated accumulating products primarily contained an A, although small amounts of CHOS with D on

Table 3
Properties of three well-characterized chitosanases.

Enzyme	Reference	GH family	Subsite specificity[1)]			Initial dominating tetramer[2)]	Degradation of chitosan F_A 0.31-0.32[3)]		
			-2	-1	+1		Initial rate (min^{-1})	Maximum α-value	DP of dominating end products[4)]
*Bs*Csn46A	This study	46	D/A	D/A	D/A	DDDD	8.4 x 10^3	0.31	2-3
ScCsn46A	(Heggset et al., 2010)	46	D/A	D/A	D/A	DDDD	325	0.44	1-3
SaCsn75A	(Heggset et al., 2012)	75	D/A	A/D	D	DDDA	6.5	0.27	2-4

[1)] In the cases where both A- and D-units productively bind to a subsite, the preferred sugar is printed in a larger font. Note that the enzymes show subtle variations in subsite specificity that are not visible in this Table; more details can be found in the References. [2)] *Bs*Csn46A, F_A = 0.30 chitosan, α = 0.11; ScCsn46A, F_A = 0.32 chitosan, α = 0.10; SaCsn75A, F_A = 0.31 chitosan, α = 0.07. [3)] the chitosans used had slightly varying F_A, as indicated in footnote 2. [2)] The range shown comprises the highest peak in the SEC chromatogram and its two neighbouring peaks. In the case of *Bs*Csn46A, no monomer was detected whereas the tetramer peak was very low; hence a range of 2–3.

the reducing end were also observed (Table 2). Similarly, di-acetylated CHOS (D1A2, D2A2) also primarily showed a dominance of acetylated reducing ends (Table 2). Apparently, the −1 subsite of this chitosanase can harbor an A quite well, as also shown by the ^{1}H NMR data for samples with α > 0.1 (Fig. 1). MS2 analysis of DP5 and DP6 CHOS was not performed due to the complexity of these samples.

The sequencing data do not allow firm statements concerning residue preferences in the +1 subsite (i.e. the subsite where the non-reducing end of a to-be formed intermediate product binds). Still, the fact that partially acetylated products accumulating early in the reaction tend to have an A at their reducing end and a D at their non-reducing end suggests that the +1 subsite has a stronger preference for D than the −1 subsite.

3.5. Substrate positioning in the active site of BsCsn46A

The preferred productive binding modes of *Bs*Csn46A were studied by degradation of $(GlcN)_5$ and $(GlcN)_6$ in $H_2{}^{18}O$ followed by product detection using MALDI-TOF-MS (Fig. 5). Product analysis was carried out when approximately 20% of the substrate was converted, and reactions were set up such as to minimize reaction and sample handling times to prevent anomeric equilibrium being reached. During the hydrolysis reaction, an ^{18}O atom is incorporated into the anomeric center (C1) of the newly formed reducing end, i.e. the sugar bound in subsite −1. Short reaction and sample handling times are needed because, due to the anomeric equilibrium, eventually all reducing ends will carry ^{18}O (Hekmat et al., 2010). Comparison of the ratios of otherwise identical ^{18}O- and ^{16}O-containing products in the MALDI-TOF MS analysis will therefore provide insight into how the substrate was bound while being cleaved. The trimer generated from $(GlcN)_5$ was almost exclusively $(GlcN)_3$ ^{18}O (Fig. 5, right panel) indicating that the productive binding mode is mainly from subsite −3 to +2 (Fig. 6, upper panel). For $(GlcN)_6$, the mass spectrometry data indicated three productive binding modes, from subsite −4 to +2, −3 to +3 and −2 to +4. It must be noted that, while we use “subsite −4” and “subsite +4” for convenience, such subsites, extending beyond subsites −3 to +3, have not been described for GH46 chitosanases and are thus hypothetical; these “subsites” may in fact be regions of weak affinity for the substrate rather than true subsite-like binding pockets for a sugar unit. Comparison of the signals for $(GlcN)_4$-^{18}O and $(GlcN)_4$-^{16}O indicates that productive binding in subsites −4 to +2 is more common than productive binding in subsites −2 to +4, with an approximate 60:40 ratio (Fig. 6, lower panel). Thus, there seems to be some difference in substrate binding affinity between these hypothetical −4 and +4 subsites. Equal amounts of $(GlcN)_3$-^{16}O and $(GlcN)_3$-^{18}O indicate productive binding of $(GlcN)_6$ to subsites −3 to +3. While it is not possible to make a direct quantitative comparison of the three binding modes (since the MS is not fully quantitative), the data shown in Fig. 5 suggest that the three binding modes, involving subsites −4 to +2, −3 to +3 or −2 to +4, have quite similar frequencies.

To our knowledge the present study is the first example of subsite mapping in a chitosanase using ^{18}O-labeled water.

4. Conclusions

*Bs*Csn46A can efficiently convert chitosans with different degrees of acetylation into mixtures of CHOS with varying chain lengths and compositions, depending on the substrate and the reaction conditions. There are clear functional differences between *Bs*Csn46A and other chitosanases, including the well-characterized and closely related ScCsn46A and a clearly different enzyme from the GH75 family, SaCsn75A. Several of these differences are discussed above and Table 3 provides a summary of key properties of the three enzymes, which all act in a non-processive endo fashion. Importantly, *Bs*Csn46A is easy to produce (Pechsrichuang et al., 2016) and displays high specific activity. Thus, as suggested before, this enzyme seems a useful tool for industrial conversion of chitosans to different CHOS composition, which may have a variety of biological activities (Aam et al., 2010; Muanprasat & Chatsudthipong, 2017) and may find several applications.

Acknowledgements

This research was supported by Suranaree University of Technology (SUT), National Research Council of Thailand (NRCT) and the Office of the Higher Education Commission under NRU project. PP was supported by SUT-Ph.D. scholarship (grant no. SUT-PhD/15/2554). NMBU contributions were supported by the Research Council of Norway through grants 221576 and 247001.

Appendix A. Supplementary data

Supplementary data associated with this article can be found, in the online version, at https://doi.org/10.1016/j.carbpol.2018.01.059.

References

Aam, B. B., Heggset, E. B., Norberg, A. L., Sørlie, M., Vårum, K. M., & Eijsink, V. G. H. (2010). Production of chitooligosaccharides and their potential applications in medicine. *Marine Drugs, 8*(5), 1482–1517.

Bahrke, S., Einarsson, J. M., Gislason, J., Haebel, S., Letzel, M. C., Peter-Katalinić, J., et al. (2002). Sequence analysis of chitooligosaccharides by matrix-assisted laser desorption ionization postsource decay mass spectrometry. *Biomacromolecules, 3*(4), 696–704.

Eide, K. B., Lindbom, A. R., Eijsink, V. G. H., Norberg, A. L., & Sørlie, M. (2013). Analysis of productive binding modes in the human chitotriosidase. *FEBS Letters, 587*(21), 3508–3513.

Fukamizo, T., Ohkawa, T., Ikeda, Y., & Goto, S. (1994). Specificity of chitosanase from *Bacillus pumilus*. *Biochimica et Biophysica Acta (BBA)/Protein Structure and Molecular Enzymology, 1205*, 183–188.

Heggset, E. B., Hoell, I. A., Kristoffersen, M., Eijsink, V. G. H., & Vårum, K. M. (2009). Degradation of chitosans with chitinase G from *Streptomyces coelicolor* a3(2): Production of chito-oligosaccharides and insight into subsite specificities. *Biomacromolecules, 10*(4), 892–899.

Heggset, E. B., Dybvik, A. I., Hoell, I. A., Norberg, A. L., Sørlie, M., Eijsink, V. G. H., et al. (2010). Degradation of chitosans with a family 46 chitosanase from *Streptomyces coelicolor* A3(2). *Biomacromolecules, 11*(9), 2487–2497.

Heggset, E. B., Tuveng, T. R., Hoell, I. A., Liu, Z., Eijsink, V. G. H., & Vårum, K. M. (2012). Mode of action of a family 75 chitosanase from *Streptomyces avermitilis*. *Biomacromolecules, 13*(6), 1733–1741.

Hekmat, O., Lo Leggio, L., Rosengren, A., Kamarauskaite, J., Kolenova, K., & Stalbrand, H. (2010). Rational engineering of mannosyl binding in the distal glycone subsites of *cellulomonas fimi* endo-β-1,4-mannanase: Mannosyl binding promoted at subsite –2 and demoted at subsite –3. *Biochemistry, 49*(23), 4884–4896.

Horn, S. J., Sørbotten, A., Synstad, B., Sikorski, P., Sørlie, M., Vårum, K. M., et al. (2006a). Endo/exo mechanism and processivity of family 18 chitinases produced by *Serratia marcescens*. *FEBS Journal, 273*(3), 491–503.

Horn, S. J., Sørlie, M., Vaaje-Kolstad, G., Norberg, A. L., Synstad, B., Vårum, K. M., et al. (2006b). Comparative studies of chitinases A, B and C from *Serratia marcescens*. *Biocatalysis and Biotransformation, 24*(1–2), 39–53.

Ishiguro, K., Yoshie, N., Sakurai, M., & Inoue, Y. (1992). A ^{1}H NMR study of a fragment of partially *N*-deacetylated chitin produced by lysozyme degradation. *Carbohydrate Research, 237*, 333–338.

Itoh, Y., Kawase, T., Nikaidou, N., Fukada, H., Mitsutomi, M., Watanabe, T., et al. (2002). Functional analysis of the chitin-binding domain of a family 19 chitinase from *Streptomyces griseus* HUT6037: Substrate-binding affinity and dominant increase of antifungal function. *Bioscience Biotechnology and Biochemistry, 66*(5), 1084–1092.

Khoushab, F., & Yamabhai, M. (2010). Chitin research revisited. *Marine Drugs, 8*(7), 1988.

Koga, D., Yoshioka, T., & Arakane, Y. (1998). HPLC analysis of anomeric formation and cleavage pattern by chitinolytic enzyme. *Bioscience Biotechnology and Biochemistry, 62*(8), 1643–1646.

Morelle, W., Canis, K., Chirat, F., Faid, V., & Michalski, J.-C. (2006). The use of mass spectrometry for the proteomic analysis of glycosylation. *Proteomics, 6*(14), 3993–4015.

Muanprasat, C., & Chatsudthipong, V. (2017). Chitosan oligosaccharide: Biological activities and potential therapeutic applications. *Pharmacology & Therapeutics, 170*, 80–97.

Pechsrichuang, P., Yoohat, K., & Yamabhai, M. (2013). Production of recombinant *Bacillus subtilis* chitosanase, suitable for biosynthesis of chitosan-oligosaccharides. *Bioresource Technology, 127*, 407–414.

Pechsrichuang, P., Songsiriritthigul, C., Haltrich, D., Roytrakul, S., Namvijtr, P., Bonaparte, N., et al. (2016). OmpA signal peptide leads to heterogenous secretion of *B. subtilis* chitosanase enzyme from *E. coli* expression system. *SpringerPlus, 5*(1), 1200.

Purushotham, P., Sarma, P. V. S. R. N., & Podile, A. R. (2012). Multiple chitinases of an endophytic *Serratia proteamaculans* 568 generate chitin oligomers. *Bioresource Technology, 112*, 261–269.

Sørbotten, A., Horn, S. J., Eijsink, V. G. H., & Vårum, K. M. (2005). Degradation of chitosans with chitinase B from *Serratia marcescens*. *FEBS Journal, 272*(2), 538–549.

Sannan, T., Kurita, K., & Iwakura, Y. (1975). Studies on chitin, 1. Solubility change by alkaline treatment and film casting. *Die Makromolekulare Chemie, 176*(4), 1191–1195.

Stefanidi, E., & Vorgias, C. E. (2008). Molecular analysis of the gene encoding a new chitinase from the marine psychrophilic bacterium *Moritella marina* and biochemical characterization of the recombinant enzyme. *Extremophiles, 12*(4), 541–552.

Takasuka, T. E., Bianchetti, C. M., Tobimatsu, Y., Bergeman, L. F., Ralph, J., & Fox, B. G. (2014). Structure-guided analysis of catalytic specificity of the abundantly secreted chitosanase SACTE_5457 from *Streptomyces* sp. SirexAA-E. *Proteins Structure Function and Bioinformatics, 82*(7), 1245–1257.

Tsukada, S., & Inoue, Y. (1981). Conformational properties of chito-oligosaccharides: Titration, optical rotation, and carbon-13NM.R. studies of chito-oligosaccharides. *Carbohydrate Research, 88*(1), 19–38.

Vårum, K. M., Antohonsen, M. W., Grasdalen, H., & Smidsrød, O. (1991). Determination of the degree of *N*-acetylation and the distribution of *N*-acetyl groups in partially *N*-deacetylated chitins (chitosans) by high-field n.m.r. spectroscopy. *Carbohydrate Research, 211*(1), 17–23.

Viens, P., Lacombe-Harvey, M.-, & Brzezinski, R. (2015). Chitosanases from family 46 of glycoside hydrolases: From proteins to phenotypes. *Marine Drugs, 13*(11), 6566.

Xia, W., Liu, P., Zhang, J., & Chen, J. (2011). Biological activities of chitosan and chitooligosaccharides. *Food Hydrocolloids, 25*(2), 170–179.